Eur. J. Biochem. 230, 733–740 (1995)

The DNA-binding domain of *Drosophila melanogaster* c-Myb undergoes a multistate denaturation

Anup MADAN, P. K. RADHA, Arvind SRIVASTAVA, Lakshmi C. PADHY and Ramakrishna V. HOSUR

Tata Institute of Fundamental Research, Bombay, India

(Received 18 December 1994/14 February 1995) – EJB 94 1895/2

The DNA-binding domain of *Drosophila* c-Myb protein has been studied using different spectroscopic probes, namely CD, fluorescence, acrylamide quenching and NMR, to determione the structure of some of its sub-domains and their relative stabilities in aqueous solutions. While CD and fluorescence spectroscopy showed that the protein had completely lost its tertiary and secondary structures in approximately 3 M urea, solvent accessibility of the tryptophan residues was still partial, as determined by acrylamide quenching. This suggested the presence of significant amounts of residual structure which persisted until the urea concentration was raised to approximately 6.0 M. Thermal-denaturation experiments also indicated the presence of an intermediate in the unfolding pathway. The experimental data could be fitted assuming a minimum of three states in both modes of denaturation. The thermodynamic parameters for the apparent three-state transition have been determined. From the protein stability curve, we have determined that *Drosophila melanogaster* Myb R123 has maximal stability at 16°C and pH 7.0.

Keywords. Myb denaturation; Myb DNA-binding domain; spectroscopic investigations; protein unfolding.

The DNA-binding domain of several myb family proteins [1, 2] are made up of three apparent repeating units (R1-R2-R3) of approximately 51–53 amino acid residues each. In each of the repeats, three conserved tryptophan residues are placed at intervals of 18/19 amino acids [3–5]. The c-myb protein binds to DNA in a sequence-specific manner [6] and various models have been proposed based upon results from Raman spectroscopy [7], site-directed mutagenesis [8] and NMR and molecular dynamics [9, 10]. Out of the three conserved stretches (R1, R2 and R3), R2-R3 has been shown to be critical for DNA binding in the chicken c-Myb protein. Recently, the secondary structures of the R3 repeat of mouse [9] and R2-R3 of chicken [10] have been determined by NMR. The results show the presence of a helix-turn-helix motif, common in many other DNA-binding proteins [11]. We have recently over-expressed the DNA-binding domain (R123) of *Drosophila melanogaster* in *Escherichia coli*. Our experimental results show that this domain forms a stable autonomously folding structural and functional unit. The protein has been found to be largely α helical, the helical content being 58.6%. Out of the nine tryptophan residues, three are solvent accessible (Madan, A., Radha, P. K., Hosur, R. V. and Padhy, L. C., unpublished results).

It has been visualized that, in proteins, the transition from the native state to the denatured state may progressively pass through states with increasing disorder [12]. Characterization of these states requires trapping them [13, 14] as they may appear transiently during the denaturation [15, 16]. However, in some proteins under conditions of partial denaturation, stable states have been shown to exist in an equilibrium [17–24]. In the recent past, there has been an increased interest in these less-ordered states, since they may play important roles in protein folding and stability, transport of proteins across membranes, proteolysis, protein modifications and turn over [23].

We present in this paper the data on the bacterially expressed DNA-binding domain of *Drosophila* c-Myb (Dm-Myb) to show that its unfolding process is more complex than a simple two-state mechanism and that one can detect significant amounts of residual structure under an apparent denatured state of the protein.

Correspondence to R. V. Hosur or L. C. Padhy, Tata Institute of Fundamental Research, Homi Bhabha Road, Colaba, Bombay 400 005, India

Fax: +91 22 2152182.

Abbreviations. TNS, 6-(*p*-toludino)-2-napthalene sulfonate; Dm, *Drosophila melanogaster*.

MATERIALS AND METHODS

Materials. Molecular-mass markers, ammonium sulfate, polyethyleneimine, isopropyl β-D-thiogalactopyranoside, 6-(*p*-toluidino)-2-naphthalene sulfonate (TNS), spectroscopic-grade dimethylsulfoxide, acrylamide, SDS, SP-Sephadex, Mops, Hepes and Mes were purchased from Sigma. DE 52 was from Whatmann and culture media were from Difco. Ultra-pure urea for denaturation experiments was obtained from Schwarz and Mann. Spectroscopic-grade ethylene glycol was obtained from Fluka. All other reagents were of analytical grade. TNS was dissolved in *N,N*-dimethyl formamide and the concentration of the stock solution was determined to be 170 mM by absorbance measurement using a molar absorption coefficient of 1.89×10^4 at 317 nm.

Protein preparation. The DNA-binding domain of the Dm-Myb was over expressed in *E. coli* and purified as described (Madan, A., Radha, P. K., Hosur, R. V. and Padhy, L. C., unpublished results). The purity of the protein was checked elsewhere by 15% SDS/PAGE [26] and was found to be greater than 95%. Protein concentration was determined by UV absorption, as suggested recently [27].

Protein unfolding. CD, fluorescence and NMR spectroscopy were used for monitoring the protein unfolding process.

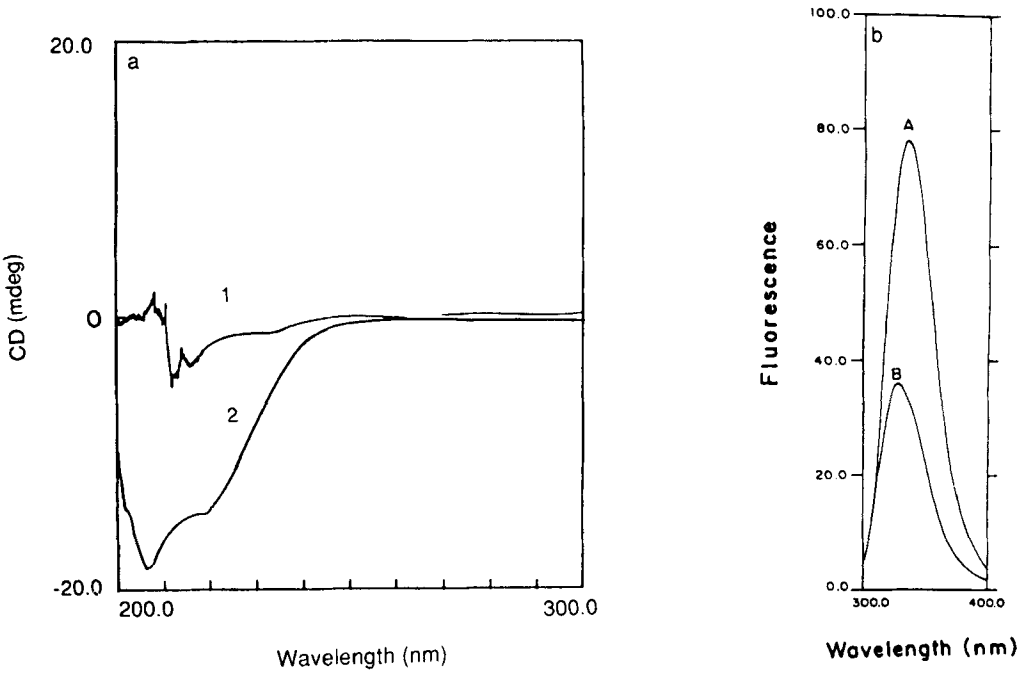

Fig. 1. CD and fluorescence characteristics of Dm-Myb R123. (a) CD spectra of the native (2) and the denatured (1) DNA-binding domain of *D. melanogaster* c-Myb (Dm-Myb R123) expressed in *E. coli* in 10 mM Tris/HCl, pH 7.0, at 25 °C. The protein concentration was 90 μM and for denaturation the spectra were recorded in the presence of 8 M urea. (b) Fluorescence emission spectra of 9 μM native (B) and denatured (A) Dm-Myb R123 in 10 mM Hepes, pH 7.0, at 25 °C. The sample was excited at 295 nm. In both cases, the spectra were corrected by subtraction of the response of the buffer alone.

For urea denaturation experiments, protein samples were incubated for at least 30 min at 25 °C at each urea concentration prior to making measurements. The experiments were performed at three different protein concentrations, 90, 105 and 125 μM and, in each case, both unfolding (increasing urea concentration) and folding (decreasing urea concentration) processes were monitored. For temperature denaturation, the samples were incubated for 15 min at each temperature, prior to making measurements. The incubation times were sufficient as no changes were observed in the fluorescence and CD spectra after these times. Under these experimental conditions, the protein unfolding was found to be reversible.

Fluorescence studies. Fluorescence measurements were made on a Shimadzu RF540 spectrofluorimeter. The band pass of both the excitation and emission monochromators was 5 nm. All measurements were carried out using 1-cm path-length cuvettes. For collection of the protein fluorescence spectra, the samples were excited at 295 nm and the spectra were corrected for the response of the buffer alone. For denaturation experiments, the fluorescence intensity at 340 nm was monitored as a function of the urea concentration.

The fraction of the tryptophan residues exposed as the protein unfolds was studied using the neutral quencher acrylamide. The changes in the protein fluorescence due to acrylamide quenching at 340 nm at various urea concentrations were monitored, and the data was analyzed according to the Lehrer equation [28]:

$$\frac{F_o}{F_o - F} = \frac{1}{f_a k_q \tau_o [Q]} + \frac{1}{f_a}, \quad (1)$$

where F_o and F are the fluorescence intensities of the protein in the absence and presence of the quencher, respectively. f_a is the fraction of quenchable fluorescence, k_q is the rate constant for quenching, τ_o is the fluorescence life time of the fluorophores in the absence of the quencher.

TNS, a probe for hydrophobic pockets [29–33], was used to monitor the stability of its only binding site on R123. The changes in the fluorescence intensity of TNS at 426 nm were monitored on exciting the protein-TNS complexes at different urea concentrations. The samples were excited at 326 nm.

CD spectroscopy. CD measurements were made on a Jasco J600 spectropolarimeter. Denaturation was monitored by changes in the intensity of the CD band at 222 nm. For each spectrum, ten scans were recorded and averaged. Each spectrum was recorded in 0.2-nm wavelength increment and the signal was acquired for 1.0 s at each wavelength. For thermal denaturation, thermostatically controlled cuvettes were used and the temperature was maintained with the help of a LKB Multitemp II thermostatic circulator.

NMR spectroscopy. NMR spectra were recorded on a Bruker AMX 500 spectrometer operating at 500 MHz for ^1H. The samples consisted of 5 mM protein in H_2O at pH 4.8. Two-dimensional clean total correlated [34] spectra were recorded with 2048 t_2 points for each of 512 t_1 points, where t_1 and t_2 are the usual time variables of two-dimensional spectroscopy. The water signal was partially suppressed by presaturation. The spin-lock mixing time was 80 ms in all the cases.

RESULTS

We have used a variety of spectroscopic techniques and strategies to derive information on the unfolding process of Dm-Myb R123. Fig. 1 shows the CD and fluorescence spectra of the native and denatured proteins. The CD spectrum (Fig. 1a) of the native protein shows two bands at 208 nm and 222 nm, characteristic of a helical structure. Urea denaturation results in significant changes in the CD spectrum. Similarly, in the fluorescence emission spectra (Fig. 1b), urea denaturation is accompanied by

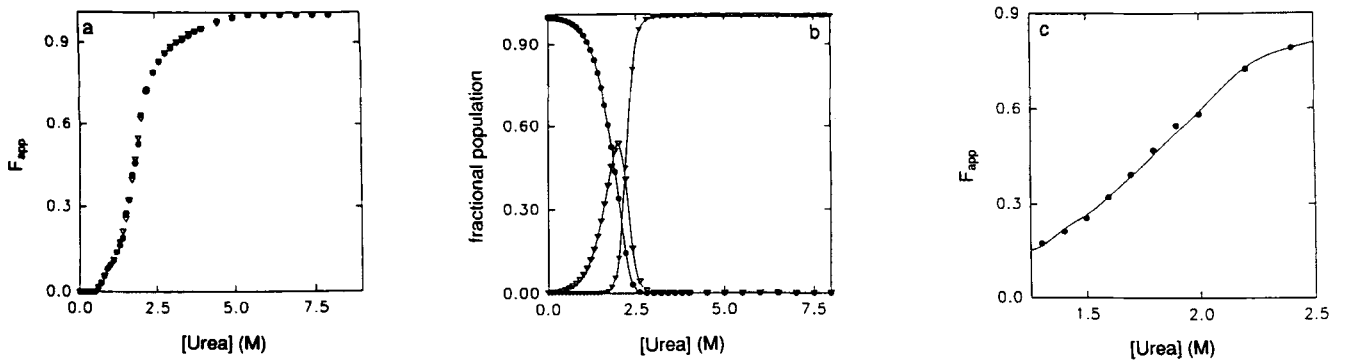

Fig. 2. Urea denaturation of Dm-Myb R123. (a) Denaturation profile of 90 μM Dm-Myb R123 in 10 mM Tris/HCl, pH 7.0, with increasing urea concentrations, monitored by changes in ellipticity (▽) at 222 nm or in fluorescence intensity (●) at 340 nm. Samples were incubated at the desired urea concentration for 30 min prior to measurement. The apparent fractional change (F_{app}) at various urea concentration was calculated according to Eqn (2). (b) Fractions of the native (●), intermediate (▽) and unfolded forms (▼) of the Dm-Myb R123 as a function of the urea concentration at pH 7.0. The various fractions were calculated from the equilibrium constants determined by the fitting of the urea denaturation curve by a three-state model. (c) Fitting of the transition region of the curve in (a) to a three-state denaturation model. The calculated curve is shown by a solid line; (●) represents the experimental data points.

Table 1. Parameters for the three-state fits. All parameters were determined from three independent experiments employing protein concentrations of 90, 105 and 125 μM, respectively. CD, fluorescence and TNS fluorescence parameters were determined from the urea denaturation curve. The temperature denaturation monitored by CD spectroscopy was at pH 7.0.

Method used	$\Delta G_i^{H_2O}$	$\Delta G_u^{H_2O}$	$\Delta G_{total}^{H_2O}$	Δn_i	Δn_u	ΔH_1	ΔS_1	ΔH_2	ΔS_2	t_{m1}	t_{m2}
	kJ/mol					kJ/mol				°C	
CD	1.5 ± 0.2	4.6 ± 0.3	6.1 ± 0.5	35	10						
Fluorescence	1.6 ± 0.2	4.7 ± 0.2	6.3 ± 0.4	35	11						
TNS fluorescence	1.2 ± 0.4	5.0 ± 0.3	6.2 ± 0.7	34	11						
Temperature denaturation by CD						194.5 ± 10.0	0.60 ± 0.03	136.3 ± 7.0	0.4 ± 0.2	47.5	66.5

a red shift from 340 nm to 350 nm and an increase in the fluorescence intensity.

Urea-induced protein denaturation. Urea-induced unfolding of the protein was reversible at all three protein concentrations used, and the profiles obtained by both CD and fluorescence were similar in all the cases. Fig. 2a shows a typical unfolding profile as a plot of F_{app} as a function of the urea concentration, where F_{app} is given by the equation:

$$F_{app} = \frac{Y_{obsd} - Y_n}{Y_u - Y_n}, \quad (2)$$

where Y_{obsd} is the observed value of the parameter (fluorescence or ellipticity) at a given urea concentration. Y_n and Y_u are the values of the parameters for the native and the unfolded proteins, respectively. The values of Y_n and Y_u are obtained by linear extrapolation of the pre-transition and post-transition regions [35]. All such curves corresponding to the three different protein concentrations have been analyzed. Only one such analysis is presented here explicitly.

The typical unfolding curve shown in Fig. 2a represents data points from two independent modes of observation (CD and fluorescence) employing the same protein concentration and using the same range of urea concentration. The profiles of unfolding in both the cases lead to similar results. Additionally, it was possible to retrace the path of unfolding when the protein in 8 M urea was progressively diluted to initiate and propagate the folding process. These results suggest that the folding/unfolding of Dm-MybR123 can be treated as thermodynamically reversible. Inspection of the unfolding curve shows an apparent biphasic transition; a relative slow phase until approximately 2.0 M urea followed by a more rapid phase at 2.0−5.0 M urea. Initial attempts to explain the data on the basis of a two-state model was unsatisfactory. A quantitative analysis of the transition region of the data of Fig. 2a was, however, possible by a three-state model:

$$N \overset{K_i}{\longleftrightarrow} I \overset{K_u}{\longleftrightarrow} U,$$

where N, I and U represent native, intermediate and unfolded states, respectively. According to this model, an equation for F_{app} can be derived following [12] and is given by:

$$F_{app} = f_n K_u \left(1 + \frac{d_i K_i}{K_u}\right), \quad (3)$$

where f_n is the fraction of the native species present at the urea concentration at which the spectroscopic parameter is measured and d_i is given by the equation

$$d_i = \frac{Y_i - Y_n}{Y_u - Y_n}, \quad (4)$$

where Y_n, Y_u and Y_i are the values of the parameters for the native, the unfolded and the intermediate states, respectively, of the protein at a given urea concentration. K_i and K_u are the equilibrium constants which are given according to the 'denaturation binding model' [12], as

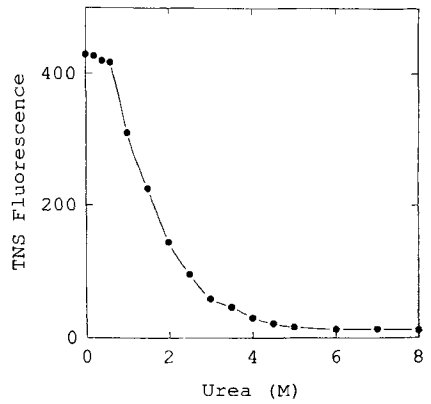

Fig. 3. Changes in the TNS fluorescence as a function of the urea concentration. *7.0 μM* protein was incubated at the desired urea concentration for 30 min. TNS was added to a final concentration of 25 μM in each sample and the emission spectra were recorded on exciting the sample at 326 nm. The changes in fluorescence intensity were monitored at 435 nm.

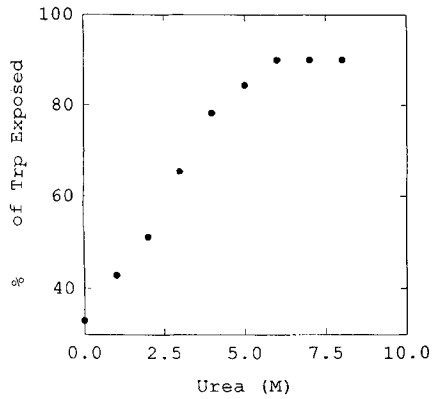

Fig. 4. Tryptophan residues exposed, determined by fluorescence quenching by acrylamide. 9 μM Dm-Myb R123 protein in 10 mM Hepes, pH 7.0 was incubated at the desired urea concentration for 30 min prior to any measurement. The changes in the fluorescence intensity at 340 nm were monitored with increasing concentrations of acrylamide at the desired urea concentration. The data were analyzed according to Eqn 1 and, from the intercept, the fraction of tryptophan residues accessible to the acrylamide was calculated for each urea concentration.

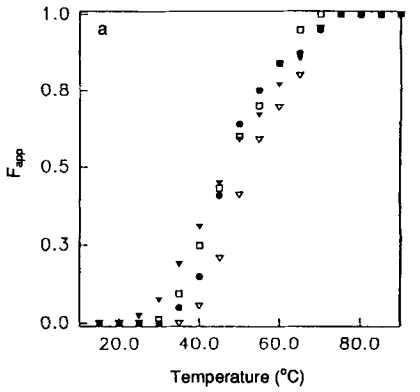

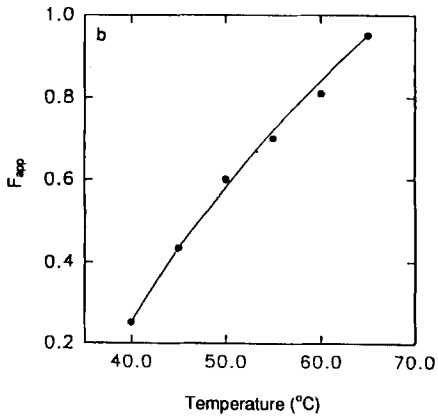

Fig. 5. Thermal denaturation of the Dm-Myb R123. Thermal denaturation curves were obtained by monitoring the changes in the CD spectra at 222 nm using a protein concentration of 90 μM in 10 mM potassium acetate, pH 4.0, (●), 10 mM potassium phosphate, pH 5.0, (□), 10 mM potassium phosphate, pH 6.0, (▼) and 10 mM Mops, pH 7.0, (▽). The apparent fractional change (F_{app}) at various temperatures was calculated according to Eqn 2. (b) Fitting of the transition region of the experimentally observed thermal denaturation curve (pH 7.0) to a three-state curve (solid line); (●) represents the experimental data points (a).

$$K_i = K^{H_2O}(1 + 0.1\,\delta)^{\Delta n_i}, \quad (5)$$

and

$$K_u = K^{H_2O}(1 + 0.1\,\delta)^{\Delta n_u} \quad (6)$$

where δ is the activity of urea, K^{H_2O} is the equilibrium constant in the absence of urea, Δn_i is the difference in the number of binding sites for urea between intermediate and native forms of the protein and Δn_u is the difference in the number of binding sites for urea between unfolded and intermediate forms of the protein.

Fig. 2c shows the fit between calculated and experimental (CD) F_{app} profiles as a function of the urea concentration. The fit is good, indicating that the three-state model is fairly adequate to describe the experimentally observed denaturation process. Similarly, the data obtained from fluorescence could be fitted to a three-state transition. The various parameters obtained by fitting experimental data from both the spectroscopic probes are listed in Table 1. Fig. 2b shows the populations of the native, intermediate and unfolded states calculated from the above parameters, as a function of urea concentration.

Molecular changes accompanying urea-induced unfolding. In a previous study, we have documented that the Dm-Myb R123 binds to a single molecule of the environmentally sensitive probe, TNS. It was further shown that the bound TNS was surrounded by four or five tryptophan residues and at least one tyrosine residue [36]. Thus, TNS was bound to a hydrophobic site contributed by more than one of the Myb repeating units as a result of its tertiary structure. We have, therefore, attempted to evaluate the stability of this TNS-binding 'hydrophobic site' as a function of the urea concentration. Since TNS remains fluorescent in only its protein-bound state, the loss of the TNS fluorescence was monitored to indicate unfolding of this sub-domain. The results presented in Fig. 3 show that urea indeed destabilized this hydrophobic sub-domain as its concentration was progressively increased. The rate of loss of TNS fluorescence closely mirrored the appearance of the unfolding intermediate.

These results seem to indicate that nearly 90% of unfolding has occurred at a urea concentration of approximately 3 M (Figs 2 and 3). To further investigate the molecular changes as-

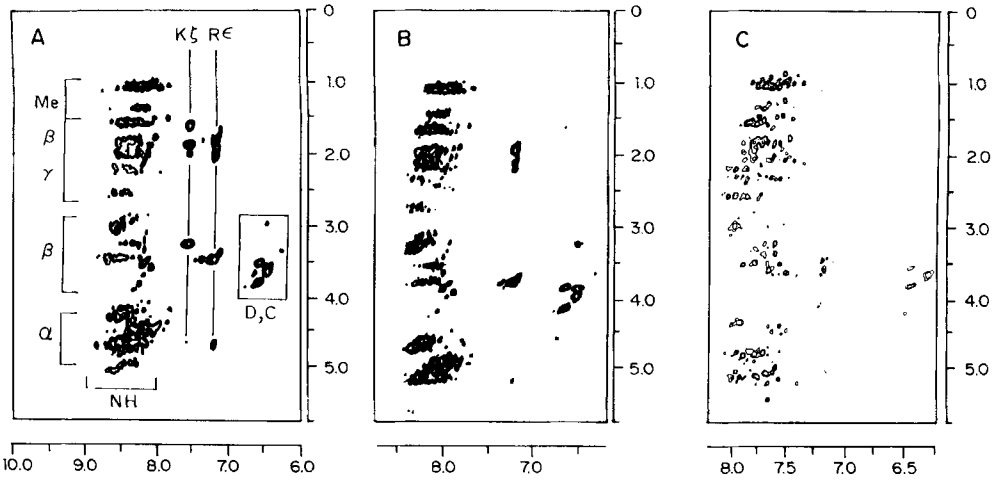

Fig. 6. Portions of the clean total correlation spectra in H_2O at temperatures 16 (A), 40 (B) and 80°C (C). All the cross peaks originate from the NH protons and gross identifications are given in (A). Single-letter symbols identify the amino acid types and Greek symbols α, β, γ, etc. identify particular proton types in the amino acids. Particularly important are the Kε and Rδ, which correspond to the side chain amino protons.

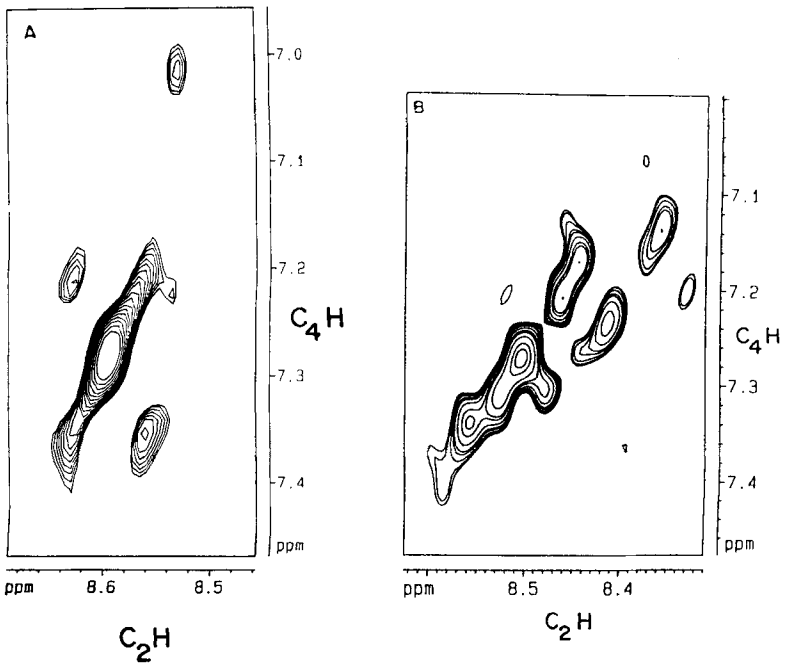

Fig. 7. C_2H-C_4H cross peaks in the clean total correlation spectra of Dm-Myb R123 in ^2H_2O at 16°C (A) and 80°C (B). 12 distinct peaks are identified in the spectrum at 80°C.

sociated with the progressive denaturation, we have monitored the solvent accessibility index of the tryptophan residues as determined from the acrylamide quenching experiments at various urea concentrations. These are presented in Fig. 4. Unlike the cases of CD, fluorescence and TNS, the tryptophan residues are exposed to the solvent rather differently. For instance, at urea concentration approximately 3.0 M, CD, fluorescence and bound TNS all show essentially a complete loss of tertiary and secondary structures, yet the extent of accessibility of tryptophan residues to the quencher remains only at 67%. It was ascertained hat this different result from collisional quenching was not an artifact due to the presence of urea by control experiments where measurements of free tryptophan fluorescence quenching in urea solutions of similar concentration ranges showed no tangible effects. Our data, therefore, leads to the conclusion that some structure is still maintained in 3–6 M urea which could not be detected by other techniques. These observation may be interpreted as suggesting that the unfolding transitions detected by quencher accessibility are probably fundamentally different from the unfolding transitions detected by CD, fluorescence and the bound TNS. This contention is further supported by the observation that the transition shown in Fig. 4 is very complex as it could not be quantified by models involving as many as four states. Nonetheless, this transition was found to be reversible over the entire range of urea concentrations, without any hysteresis. Thus, the exposure of tryptophan residues to the quencher documents a finer dissection of the transition process involving several potential intermediate states and extends the range of urea concentration over which the protein actually unfolds.

Thermal unfolding of Dm-Myb R123. We monitored the changes in the intensity of the CD band at 222 nm as a function

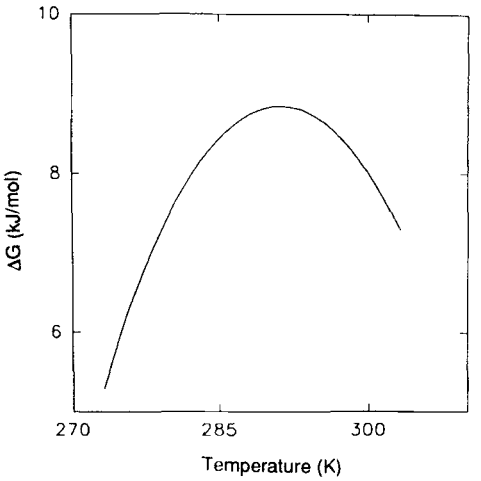

Fig. 8. Stability of the native state. Unfolding free energy as a function of temperature at pH 7.0, calculated from Eqn 8. The curve has a maximum at 16°C, indicating that the protein has maximum stability at this temperature.

of the temperature for three different protein concentrations in the pH range 4–7. Again, the unfolding of Dm-Myb R123 was found to be reversible in each case. Typical unfolding profiles are presented in Fig. 5a. The unfolding profile in the transition zone of Fig. 5a could be adequately explained with the invocation of a three-state model. A typical three-state fit of the experimental data points at pH 7.0 is shown (Fig. 5b) and the various parameters of the fits are listed (Table 1). For this non-linear fitting, we assumed that the enthalpy changes (ΔH) and the entropy changes (ΔS) are not explicitly dependent on temperature in the transition region. It is interesting to note that the standard enthalpy changes for the transitions in this analysis are similar to those obtained by Sarai et al. [37] by differential scanning calorimetery on the mouse R123. This similarity (within 20%) of ΔH values might indicate that similar kinds of structural transitions occur in *Drosophila* R123 and mouse R123 proteins. Table 1 also indicates that for native to intermediate and intermediate to denatured transitions, both ΔH and ΔS terms make nearly equal contributions.

We further used NMR spectroscopy to gain some insight into the molecular aspects of unfolding process. Fig. 6 shows portions of two-dimensional clean total correlation [34] spectra at pH 4.8, containing cross peaks belonging to various NH (both back bone and side chain) protons in the protein at three different temperatures, 16, 40 and 80°C. The different regions of the cross peaks have been identified (Fig. 6A). However, for the present, we focus attention on the peaks belonging to the side chains of the lysine and arginine residues which appear distinctly from the other NH protons [38]. We notice that, as the temperature is increased, the lysine peaks disappear (at 40°C) whereas those of arginine residues remain, indicating that lysine residues become accessible to the solvent faster than the arginine residues. At 80°C, both the lysine and the arginine peaks have disappeared completely. It is clear that the lysine interactions are relatively weak compared to arginine interactions and that some of the intermediates in temperature denaturation likely arise from loss of stability contributions from lysine residues.

Comparison of two-dimensional clean total correlation spectral regions [34] of the protein showing C_2H-C_4H cross peaks of the histidine imidazole rings of Dm-Myb R123 at 16°C and 80°C (Fig. 7) shows clear differences. The state attained at 80°C is such that some order is still present. For example, at 80°C 12 peaks are seen as against six expected for the six histidine residues. This indicates that there are at least two structures in equilibrium with sizeable populations in the thermal 'denatured' state.

The stability of the native state. Determination of conformational stability of the native protein requires the calculation of the Gibb's free energy difference between the native and the unfolded state. This is a function of temperature and can be calculated by the Gibbs-Helmholtz equation:

$$\Delta G(T) = \Delta H_n [1 - (T/T_n)] - \Delta C_p[(T_n - T) + T \ln (T/T_n)], \quad (7)$$

where ΔC_p is the difference in the heat capacities of the folded and the unfolded states, ΔH_n is the enthalpy change at temperature T_n. At T_n = transition temperature (T_m), for which ΔH has already been determined, Eqn (7) can be rewritten as

$$\Delta G(T) = \Delta H_m [1 - (T/T_m)] - \Delta C_p [(T_m - T) + T \ln (T/T_m)]. \quad (8)$$

Here, ΔC_p has been assumed to be independent of temperature. In order to assess the validity of this assumption, we adopted the procedure suggested by Pace and Laurents [39] and determined ΔC_p values at different temperatures. These were found to be 6.10, 6.27 and 6.57 kJ · mol^{-1} · cm^{-1} · K^{-1}, respectively, at 5, 10 and 15°C. Since the estimated experimental errors in the measurements were 5–10%, we concluded that the observed variations in ΔC_p were within the experimental errors; this meant that ΔC_p could be considered to be constant in the temperature range 0–30°C. A similar observation has also been made in the case of mouse R123 [37], where C_p values were measured by differential scanning calorimetery. Taking an average value of ΔC_p from the above measurements, $\Delta G(T)$ was calculated theoretically at different temperatures in the temperature range 0–30°C; this is shown in Fig. 8. This is referred to as the 'protein stability curve' [40] and indicates that the protein has maximum stability around 16°C; the curve has a maximum positive ΔG at this temperature.

DISCUSSION

Our results have showed that the unfolding of Dm-Myb R123 is a complex process involving several states. Unfolding in the range 0–3 M urea is characterized by a process involving at least one intermediate which becomes predominant (at approximately 2.0 M urea) in the three-state equilibrium. As far as CD, fluorescence and TNS are concerned, the unfolding process is essentially complete in 3.0 M urea. The loss of helical structure found in our experiments was concomitant with the loss of the TNS fluorescence. Thus, it was imperative that the integrity of the TNS-binding site was in direct correlation with the integrity of the helices present in the R123 structure. Since TNS in its bound state probed the integrity of a relatively specific and a small region of the protein, we expected TNS-urea experiments to allow a finer dissection of the unfolding process but this was not seen.

Experiments designed to quantify the accessibility of the tryptophan residues to the neutral quencher acrylamide present a profile of unfolding which is different from the three other modes. In this case, at 3.0 M urea only 67% of the tryptophan residues were accessible to the quencher, while other methods recorded an apparent completion of the unfolding process. It was not until the urea concentration was raised to nearly 6.0 M that the exposure of the tryptophan residues to the quencher reached near completion. The reversibility of this process underscores the potential importance of the path during protein refolding.

Although residual structures for the denatured proteins have been recorded before [41–46], our results provide another compelling example.

In the thermal unfolding of Dm-Myb R123, we again found that more than two states are necessary to explain the transition at each of the four discrete pH values used. From NMR, we observed that some of the residues display order even at fairly high temperatures. Notably, histidine residues are components of an ordered structure surviving at 80 °C, testifying the presence of long-range interactions and making a case for these histidine residues scattered among all the three repeats to be their mediators.

Finally, we have evaluated the heat capacity parameters for the Dm-Myb R123 protein from the unfolding transition, which allows the computation of thermodynamic parameters of stability. The results show that the protein has maximal stability at 16 °C and at pH 7.0.

The facilities provided by the 500 MHz FT NMR National Facility supported by the Department of Science and Technology, Government of India, and located at T. I. F. R., Bombay are gratefully acknowledged. We thank P. N. Bhavsar for helpful suggestions. LCP thanks the Lady Tata Memorial Trust for the financial support.

REFERENCES

1. Luscher, B. & Eisenman, R. (1990) New light on Myc and Myb. Part 2, *Myb Genes & Dev. 4*, 2235–2240.
2. Shen-Ong, G. L. C. (1990) The Myb Oncogene, *Biochem. Biophys. Acta 1032*, 39–52.
3. Klempnauer, K.-H. & Sippel, A. E. (1987) The highly conserved amino-terminal region of the protein encoded by the v-Myb oncogene functions as a DNA-binding domain, *EMBO J. 6*, 2719–2725.
4. Howe, K. M., Reakes, C. F. L. & Watson, R. J. (1990) Characterization of sequence specific interaction of mouse c-myb protein with DNA, *EMBO J. 9*, 161–169.
5. Biedenkapp, H., Borgmeyer, U., Sippel, A. E. & Klempnauer, K.-H. (1988) Viral myb oncogene encodes a sequence specific DNA binding activity, *Nature 335*, 835–837.
6. Nakagoshi, H., Nagase, T., Kanei-Ishii, C., Ueno, Y. & Ishii, S. (1990) Binding of the c-myb proto-oncogene product to the Simian Virus 40 enhancer stimulates transcription, *J. Biol. Chem. 265*, 3479–3483.
7. Kanei-Ishii, C., Sarai, A., Sawazaki, T., Nakagoshi, H., He, D.-N., Ogata, K., Nishimura, Y. & Ishii, S. (1990) The tryptophan cluster: A hypothetical structure of the DNA-binding domain of the myb proto-oncogene product, *J. Biol. Chem. 265*, 19990–19995.
8. Frampton, J., Gibson, T. J., Ness, S. A., Doderlein, G. & Graf, T. (1991) Proposed structure for the DNA-binding domain of the Myb oncoprotein based on model building and mutational analysis, *Prot. Eng. 4*, 891–901.
9. Ogata, K., Hojo, H., Aimoto, S., Nakai, T., Nakamura, A. S., Ishii, S. & Nishimura, Y. (1992) Solution structure of a DNA binding unit of Myb: A helix-turn-helix related motif with conserved tryptophans forming a hydrophobic core, *Proc. Natl Acad. Sci. USA 89*, 6428–6432.
10. Jamin, N., Gabrielsen, O. S., Gilles, N., Lirsac, P.-N. & Toma, F. (1993) Secondary structure of the DNA-binding domain of c-Myb proto-oncogene in solution. A multi dimensional double and triple heteronuclear NMR study, *Eur. J. Biochem. 216*, 147–154.
11. Steitz, T. A. (1990) Structural studies of protein-nucleic acid interaction: the sources of sequence-specific binding, *Quart. Rev. Biophys. 23*, 205–280.
12. Tanford, C. (1970) Protein Denaturation, Part C, Theoretical Models for the mechanism of denaturation, *Adv. Prot. Chem. 24*, 1–95.
13. Kim, P. S. (1986) Amide proton exchange as a probe of protein folding pathways, *Methods Enzymol. 131*, 136–156.
14. Kim, P. S. & Baldwin, R. L. (1990) Intermediates in the folding reactions of the small protein, *Annu. Rev. Biochem. 59*, 631–660.
15. Tanford, C. (1968) Protein Denaturation, *Adv. Prot. Chem. 23*, 121–282.
16. Kim, P. S. & Baldwin, R. L. (1982) Specific Intermediates in the folding reactions of small proteins and the mechanism of protein folding, *Annu. Rev. Biochem. 51*, 459–489.
17. Kuwajima, K. (1977) A folding model of α-lactalbumin deduced from the three state denaturation mechanism, *J. Mol. Biol. 114*, 241–258.
18. Dolgikh, D. A., Gilmanshin, R. I., Brazhinkov, E. V., Bychkova, V. E., Semisotnov, G. V., Venyaminov, S. Y. & Ptitsyn, O. B. (1981) α-lactalbumin: compact state with fluctuating tertiary structure, *FEBS Lett. 136*, 311–315.
19. Denton, J. B., Konishi, Y. & Scheraga, H. (1982) Folding of Ribonuclease A from a partially disordered conformation: kinetic study under folding conditions, *Biochemistry 21*, 5155–5163.
20. Ohgushi, M. & Wada, A. (1983) Molten globule state: a compact form of globular proteins with mobile side chains, *FEBS Lett. 164*, 21–24.
21. Brazhnikov, E. V., Chigadze, D. A., Dolgikh, D. A. & Ptitsyn, O. B. (1985) Non-cooperative temperature melting of a globular protein without specific tertiary structure, *Biopolymers 24*, 1899–1907.
22. States, D. J., Creighton, T. E., Dobson, C. M. & Karplus, M. (1987) Conformations of intermediates in the folding of Pancreatic Trypsin Inhibitor, *J. Mol. Biol. 195*, 731–739.
23. Dill, K. A. & Shortley, D. (1991) Denatured states of proteins, *Annu. Rev. Biochem. 60*, 795–825.
24. Ptitsyn, O. B. (1992) in *Protein folding* (Creighton, T. E., ed.) pp. 243–300, W. H. Freeman, New York.
25. Reference deleted.
26. Lammeli, U. K. (1970) Cleavage of structural proteins during the assembly of the head of bacteriophage T4, *Nature 227*, 680–685.
27. Mach, H., Middugh, C. R. & Lewis, R. V. (1992) Statistical determination of the average values of the extinction coefficients of tryptophans and tyrosines in native proteins, *Anal. Biochem. 200*, 74–80.
28. Lehrer, S. S. (1971) Solute perturbation of protein fluorescence: The quenching of the tryptophyl fluorescence of model compounds and of lysozyme by iodide ion, *Biochemistry 10*, 3254–3262.
29. Strickland, D. & Bhattacharya, P. (1984) Kinetics of the conformational alterations associated with nucleophilic modification of α_2-macroglobulin, *Biochemistry 23*, 3115–3124.
30. Strickland, D., Steiner, J. P., Feldman, S. R. & Pizzo, S. V. (1984) Fluorescent probes as a measure of conformational alterations induced by nucleophilic modification and proteolysis of Bovine α_2-macroglobulin, *Biochemistry 23*, 6679–6685.
31. Steiner, J. P., Bhattacharya, P. & Strickland, D. K. (1985) Thrombin induced conformational changes of human α_2-macroglobulin: evidence for two functional domains, *Biochemistry 24*, 2993–3001.
32. Steiner, J. P., Migliorni, M. & Strickland, D. K. (1987) Characterization of the reaction of plasmin with α_2-macroglobulin: effect of antifibrinolytic agents, *Biochemistry 26*, 8487–8495.
33. Lin, W. Y., Eads, C. D. & Villafranca, J. J. (1991) Fluorescent probes for measuring the binding constants and distances between the metal ion bound to *Escherichia coli* Glutamine Synthase, *Biochemistry 30*, 3421–3426.
34. Griesinger, C., Otting, G., Wuthrich, K. & Ernst, R. R (1988) Clean TOCSY for ^{1}H spin system identification in macromolecules, *J. Am. Chem. Soc. 110*, 7870–7872.
35. Schmid, F. X. (1989) in *Protein structure: a practical approach* (Creighton, T. E., ed.) pp. 251–285, IRL Press, Oxford, UK.
36. Madan, A., Hosur, R. V. & Padhy, L. C. (1994) Sequence-specific DNA displaces 6-p-toluidino-2-naphthalenesulfonate bound to a hydrophobic site on the DNA-binding domain of *Drosophila* c-myb, *Biochemistry 33*, 7120–7126.
37. Sarai, A., Uedaira, H., Morii, H., Yasukawa, T., Ogata, K., Nishimura, Y. & Ishii, S. (1993) Thermal stability of the DNA-binding domain of the Myb Oncoprotein, *Biochemistry 32*, 7759–7764.
38. Wuthrich, K. (1986) *NMR of proteins and nucleic acids*, Wiley, New York.

39. Pace, C. N. & Laurents, D. V. (1989) A new method for determining the heat capacity changes for protein folding, *Biochemistry 28*, 2520–2525.
40. Becktell, W. J. & Schellman, J. A. (1987) Protein stability curves, *Biopolymers 26*, 1859–1877.
41. Bierzynski, A. & Baldwin, R. L. (1982) Local secondary structure in Ribonuclease A denatured by guandine. HCl near 1 °C, *J. Mol. Biol. 162*, 173–186.
42. Haas, E., McWherter, C. A. & Scheraga, H. A. (1988) Conformational unfolding in the N-terminal region of Ribonuclease A detected by non radiative energy transfer: distribution of inter residue distances in the native, denatured and reduced-denatured states, *Biopolymers 27*, 1–21.
43. Shortle, D. & Meeker, A. K. (1989) Residual structure in large fragments of Staphylococcal Nuclease: effect of amino acid substitution, *Biochemistry 28*, 936–944.
44. Baun, J., Dobson, C. M., Evans, P. A. & Hartley, C. (1989) Characterization of a partly folded protein by NMR methods: studies on the molten globule state of guinea pig a-lactalbumin, *Biochemistry 28*, 7–13.
45. Kuwajima, K. (1989) The molten globule state as a clue for understanding the folding and co-operativity of globular protein structure, *Prot. Struc. Funct. Genet. 6*, 87–103.
46. Creighton, T. E. (1993) *Proteins: structure and molecular properties*, pp. 292, W. H. Freeman and Co.